



Capacitive deionization using a pulsed power supply for water treatment

Zhaoyan Jin^a, Xiaomin Hu^{a,*}, Tong Sun^a, Wenbo Zhang^b

^aSchool of Resources and Civil Engineering, Northeastern University, NO. 3-11, Wenhua Road, Heping District, Shenyang 110819, China, email: boy_jzy8764@163.com (Z. Jin), hxmin_jj@163.com (X. Hu), sun1992sy@163.com (T. Sun)

^bDepartment of analysis, Liaoning Metallurgical Geological Exploration Institute, No.60. Wuyi Road. Tiedong district, Anshan 114001, China, email: girl_zwb@163.com (W. Zhang)

Received 15 January 2019; Accepted 13 May 2019

ABSTRACT

A capacitive deionization system utilizing a pulsed power supply was designed and investigated for desalination. In most studies on capacitive deionization, direct current power supply is the most common power source. Compared with traditional direct-current capacitive deionization, pulsed-capacitive deionization exhibits some excellent properties in desalination: lower power consumption, higher removal rate. The optimal operational conditions of a pulsed power supply in capacitive deionization were discussed in this study. From the experiment results, as for NO_3^- of initial concentration 40 mg/L, a duty cycle of 50% and a frequency of 1000 Hz were optimal. From the theory of electrolyte solution, the optimal frequency is related to properties of ion, such as: ionic radius, valence, ion mobility, and also related to the concentration of ion. The results of molecular dynamics simulation were consistent with the experimental results. The reasons for excellent performances of pulsed-capacitive deionization in desalination may be that: the effect of concentration polarization and the migration resistance from solution to the EDL were reduced. Pulsed-capacitive deionization could be used for low concentration water desalination and it provides a new idea for the preparation of ultra pure water and the advanced treatment of wastewater.

Keywords: Pulsed electric field; Capacitive deionization; Molecular dynamics simulation; Hydration layer; Orientation polarization

1. Introduction

In recent years, capacitive deionization (CDI for short) has been widely used as a water purification technology in many applications, because of the advantages it provides: environmentally friendly technology, low energy consumption and the operation is simple and safe [1–3].

As CDI gets more and more attention, many studies have been carried out by scholars all around the world. Most researches are about the electrode materials (carbon aerogel, carbon nanotubes, grapheme) [4–7], integration of microbial fuel cells and CDI [8,9], membrane CDI [10,11] and flow-electrode CDI [12,13].

Typical concentration of dissolved salts in seawater and brackish water are 35,000 and 1000 mg/L [14].

In treatment of the typical seawater and wastewater, it is effective by CDI with the common activated carbon coated electrodes. However, in many of our experiments, for low concentration of saline water, such as: initial concentration <50 mg/L, a such common CDI doesn't achieve a satisfactory performance. For the desalination of such a low concentration of saline water, electro dialysis, reverse osmosis, and ion exchange are commonly used. But the energy consumption and additional cost of above technologies are high. So we would like to try to use CDI for low concentration water desalination and provide a new idea for the preparation of ultra pure water and the advanced treatment of wastewater.

The pulsed electric field is widely used in electroplating [15,16] and electro dialysis [17–19]. The principle of CDI is different from the above technologies, but under the electric field, ions transfer from solution to the electrode or the

*Corresponding author.

electro dialysis membranes, this process of the CDI, electro dialysis and electroplating are interlinked. However, there have been no reports about the direct application of pulsed power supply in CDI. In 2014, the enhancement of pulsed electrical potential was studied [20]. The neutron imaging and effective diffusion coefficient were employed for the study on the mechanism. From our point, some more could be studied in depth.

In the pulsed power supply, voltage amplitude or current amplitude, duty cycle, and frequency were the main parameters. The voltage amplitude is the parameter for output voltage (or current). The duty cycle (D) is the parameter for the ratio of loaded time (t_{on}) and unloaded time (t_{off}) in one pulsed cycle (T). Frequency (f) is reciprocal to the period, and is the parameter for the length of one pulse period as shown in Eqs. (1)–(3):

$$T = t_{on} + t_{off} \quad (1)$$

$$f = \frac{1}{t_{on} + t_{off}} \quad (2)$$

$$D = \frac{t_{on}}{t_{on} + t_{off}} \quad (3)$$

So the purpose of this paper is to study the application of the pulsed power supply in CDI. The CDI cell, including the reactor and the activated carbon coated electrode was designed. The pulsed power supply was applied in CDI for the electric field. The removal rate and energy consumption of direct current-CDI (DC-CDI for short) and pulsed- capacitive deionization (pulsed-CDI for short) were compared. The operational parameters, including duty cycle, frequency, were investigated to determine the optimal conditions. The molecular dynamics simulation (MD for short) was used to study the mechanism of pulsed-CDI.

2. Materials and methods

2.1. Pulsed-CDI system

The pulsed-CDI system, including a CDI cell, a pulsed power supply, a peristaltic pump, a power analyzer and two feed tanks, was designed in a closed-loop mode, as depicted in Fig. 1. The peristaltic pump (Shanghai QingPu, China) was used to make the water circulated in feed tank and CDI cell. The pulsed power supply (Shanghai SoYi, China) provided a unidirectional square-wave pulsed current. The waveform of pulsed current in this study is shown as Fig. 3. The power analyzer (Fluke, USA) was used to monitor current, voltage and energy consumption. The two feed tanks were used to store saline water in adsorption phase and backwash water in desorption phase with a volume of 2 L.

As shown in Figs. 2a and 2b, the CDI cell consisted of reactor and electrodes. The reactor was made of Plexiglas. The internal grooves were used to fix the electrodes. The space between grooves was 2 mm, and this space was also the distance between the electrodes. A valve was placed at the bottom of the reactor for drainage at the end of adsorp-

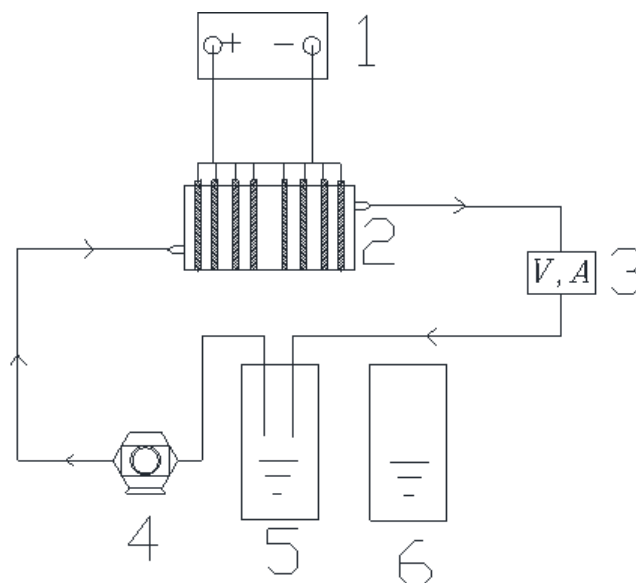


Fig. 1. Schematic diagram of pulsed-CDI system. 1. Pulsed power supply; 2. CDI cell; 3. Power analyzer; 4. Peristaltic pump; 5. Feed tank for saline water in adsorption phase; 6. Feed tank for backwash water in desorption phase.

tion or desorption stage. The electrode plate was made of titanium alloy (120 mm × 100 mm × 2 mm) as depicted in Fig. 2c. The preprocessing were as follows: after cutting down to size, the surface of titanium plate was smoothed by a sandpaper; a NaOH solution of 10% mass concentration was used to de-oil the surface at 90°C for 1 h; finally, a H₂C₂O₄ solution of 10% mass concentration was used for etching at 90°C for 1 h.

Powdered activated carbon (Fuzhou, China) was used as the electrode material. The slurry for coating, was made of activated carbon powder, polyvinylidene fluoride (PVDF for short, M.W = 275000), and conductive agent at the ratio of 25.5 : 3 : 1.5. A total of 30 g, activated carbon powder as adsorbents, PVDF as the binder, and the graphite powder as the conductive agent were mixed in dimethylacetamide (DMAc for short) solution of 100 ml. After stirring the slurry for 12 h to guarantee homogeneity, the slurry was uniformly brushed on the titanium plate by the automatic coating machine. The coated electrodes were dried in a drying oven at 60°C for 4 h and in a vacuum drying oven at 60°C for 4 h to form the coating of an approximate weight of 3.0 g and almost no remaining organic solvents [2], as depicted in Fig. 2d. In each experiment, the coating of electrode was newly prepared to ensure the same initial conditions.

Wastewater was prepared by NH₄Cl, NaNO₃ (Sino-pharm Chemical Reagent, China) in deionized water and were used as feed water. The initial concentration of NH₃-N, NO₃-N solution were 25 mg/L, 40 mg/L, respectively. The backwash water was prepared by distilled water.

2.2. Experimental methods

A CDI experimental cycle consisted of two parts: the adsorption phase (20 min) and the desorption phase (3 min). In the adsorption phase, saline water was circu-

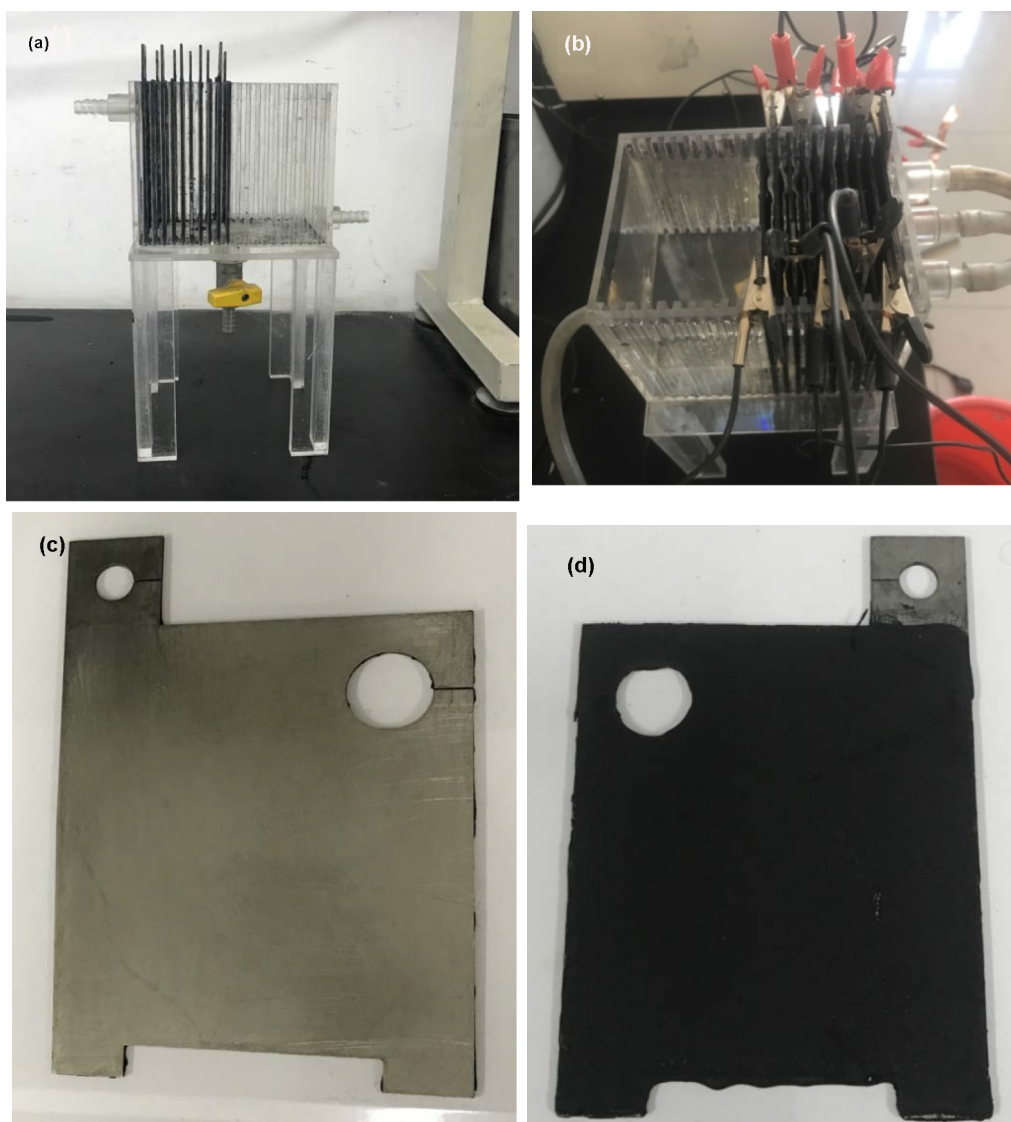


Fig. 2. CDI cell. (a) and (b); (c) and (d): electrode and coated electrode.

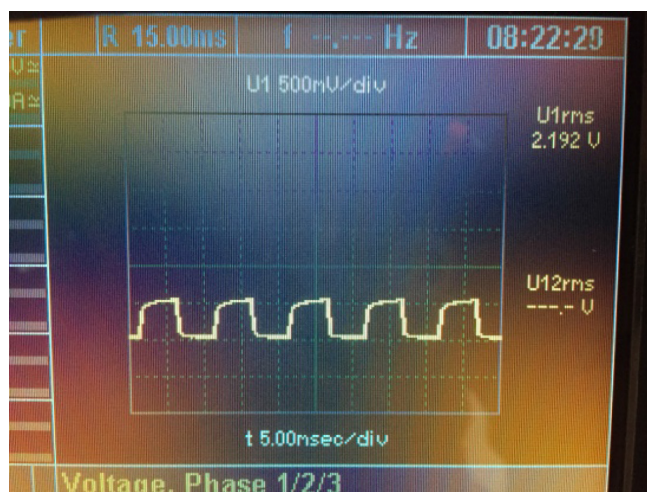


Fig. 3. Pulsed current.

larly pumped from the feed tank (5) to the CDI cell at the flow rate of 80 ml/min. After adjusting the parameters of pulsed power supply, turned on the pulsed power supply and power analyzer, lasted 20 min. The samples for test were taken every 5 min. After 20 min, turned off the peristaltic pump, and opened the valve. Until the saline water in CDI cell was drained, turned off the pulsed power supply. In the desorption phase, the method of broken connection was chosen for desorption. Switched to the feed tank (6), pumped the backwash water from the feed tank (6) to the CDI cell circularly at the flow rate of 1 L/min, after 3 min, opened the valve, the adsorbed ions are taken away by backwash water and the regeneration of electrodes was completed. The current, voltage and energy consumption were measured by the power analyzer. In this study, there were 3–5 cycles in a CDI experiment. The ion concentration of sample was tested by ion chromatography (QingDao PuRen, China). 0.8 A in the constant current mode was applied in both DC-CDI and pulsed-

CDI. The coating material in this study was common activated carbon. Details of carbon materials for CDI were described in the paper of Zhao [2], and no more discussion in this study.

The removal rate (R , %) was calculated by Eq. (4):

$$R = \frac{(c_0 - c_e)}{c_0} \times 100\% \quad (4)$$

where C_0 and C_e are the initial and equilibrium concentration (mg/L), respectively; energy consumption (E , kWh/kg) was calculated by Eq. (5):

$$E = \frac{E_t}{m} \quad (5)$$

where E_t is the energy consumption (kWh) measured by the power analyzer (Fluke, USA), and m is the mass (kg) of removal ions.

2.3. Molecular dynamics simulation

We used the molecular dynamics simulation to simulate the adsorption process of both DC-CDI and pulsed-CDI. As shown in Fig. 4, the system consists of two graphite sheets with a distance of 75 Å, 1817 water molecules and 32 Na⁺ ions (the concentration was 1 mol/L). The upper (75 Å) and lower (0 Å) graphite sheet were respectively charged with negative 0.05e and positive 0.05e. In order to simulate the DC electric field and the pulsed electric field, the charged methods were constant loading and pulsed loading, respectively [21]. In the pulsed charging mode, the duty cycle was 50%, and the frequency range was 5GHz–10THz. Although many studies are about the asymmetric capacitance behavior of anions and cations in capacitors [22], we just intended to compare the DC-CDI and the pulsed-CDI, so only Na⁺ were set in the system, the anions were not set.

Our simulations were run in LAMMPS [23]. Package with CHARMM36 force field [24] in NVT ensemble. The

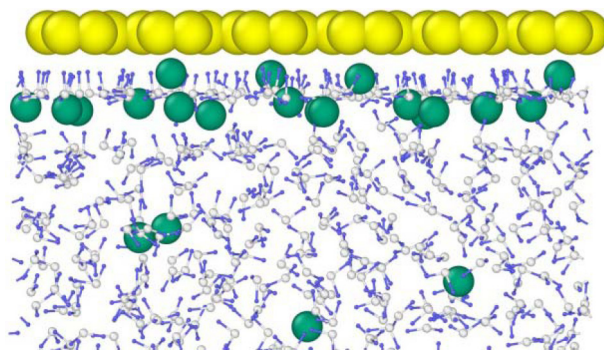


Fig. 4. Snapshot of the simulation system.

system was perpendicular to the plane of graphene sheet. The periodic boundary conditions were used in the direction parallel to the plane of graphene sheet. The TIP3P water model [25] was used. The interaction between water and carbon atoms were the same [26]. The Nosé-Hoover method was used to couple the temperature at 300 K. We used the ppm method [27] to as the electrostatic interactions. The time step was 1 fs. We collected the data every 1 ps. The cut-off of Lennard-Jones interaction was 1.05 nm. The temperature rise period before electric field loading was 1 ns. Each simulation was conducted for 20 ns.

3. Results and discussion

3.1. Performance of pulsed-CDI in desalination

3.1.1. Removal of NH₄⁺ and NO₃⁻

As shown in Fig. 5, in low-concentration saline water desalination, the removal rate of NH₄⁺ and NO₃⁻ using DC-CDI was 17.6% and 38%, while pulsed-CDI had a NH₄⁺ removal rate of 79.2% and 62%. The advantage of pulsed-CDI in desalination is evident.

In 2006, the level A standard for wastewater discharges was promulgated by the Chinese Environmental Protection

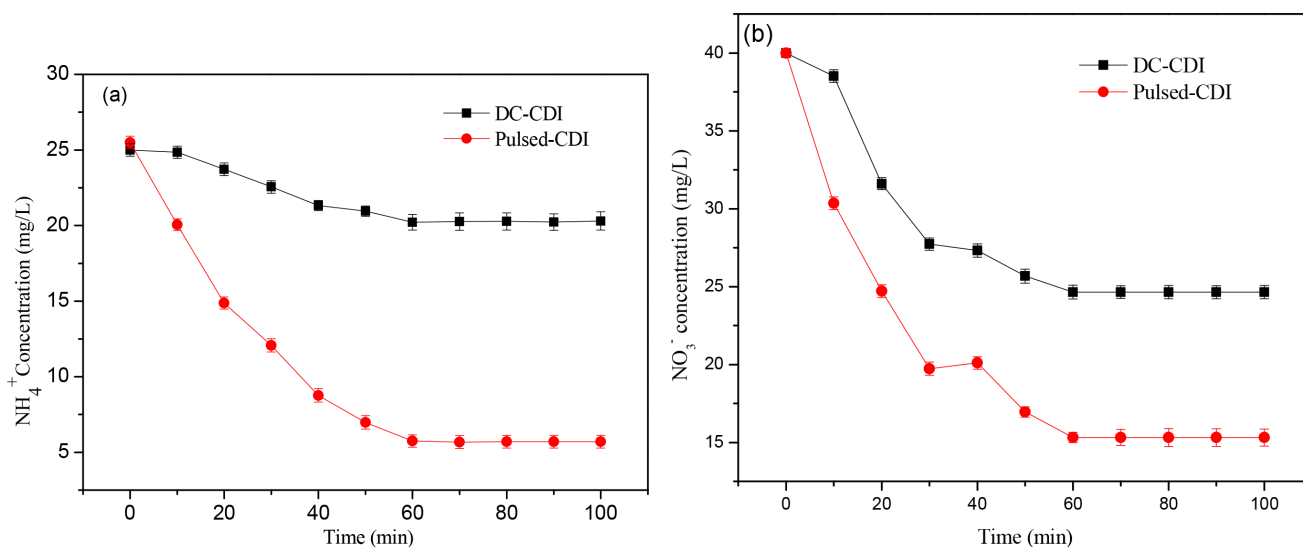


Fig. 5. Performance of DC-CDI and pulsed-CDI (a frequency of 100 Hz and a duty ratio of 50%) in desalination. (a) NH₄⁺, (b) NO₃⁻.

Agency. In level A standard, the permitted emission concentration of pollutants, such as: total nitrogen, $\text{NH}_3\text{-N}$, total phosphorus, and COD, was further reduced. For $\text{NH}_3\text{-N}$, if the temperature $> 12^\circ\text{C}$, the permitted emission concentration of $\text{NH}_3\text{-N} < 5 \text{ mg/L}$; for temperatures $< 12^\circ\text{C}$, the permitted emission concentration of $\text{NH}_3\text{-N} < 8 \text{ mg/L}$. Based on an existing sewage treatment plant in China, advanced wastewater treatment technologies are needed for level A standard. So, the pulsed-CDI may be an effective method for advanced waste water treatment.

3.1.2. Desorption stage of pulsed-CDI

The regeneration of electrode is an important step in CDI process, and it is the key to the large-scale application of CDI. In this section, three desorption methods (short connection, open circuit and reverse connection) were compared. As shown in Fig. 6, the adsorption stage was from 0 min to 30 min, and the desorption stage was from 30 min to 60 min, and the short connection was optimal regeneration method.

Each pair of electrodes in CDI could be regarded as a parallel plate capacitor and an energy storage device. When the power is cut off (open circuit), the capacitor discharges outward. It takes a period of time for the electrode to release the stored charge, and during this time, there is still voltage between the positive and negative electrode, resulting in a slow desorption.

For the reverse connection of positive and negative electrodes, it could cause a re-absorption, and it took extra energy. While for the short connection, a rapid regeneration of electrodes without extra power consumption was realized. The short connection was optimal regeneration method.

As shown in Fig. 7, after three cycles (adsorption and desorption), there wasn't an obvious decline of performance in CDI, the change trend of concentration was consistent, and the effluent concentrations of NO_3^- was 19.9 mg/L, 20.5 mg/L and 20.1 mg/L, respectively. The results showed that the operation of equipment was relatively stable.

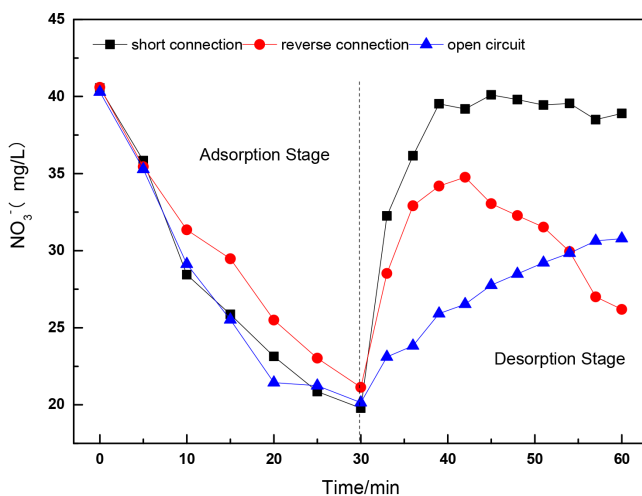


Fig. 6. Comparison of desorption method (short connection, open circuit and reverse connection).

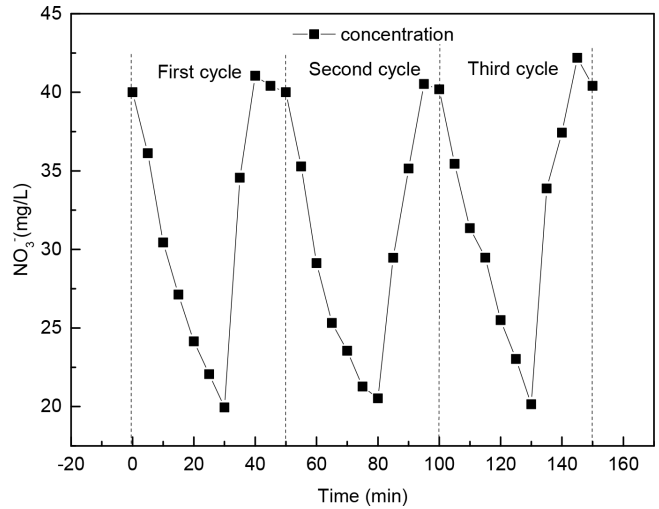


Fig. 7. Regeneration of electrode.

3.1.3. Energy consumption of DC-CDI and pulsed-CDI

Energy consumption is an important measure of a technology. In this study, the energy consumption of DC-CDI and pulsed-CDI was compared. The energy consumption for removing NO_3^- was 12.24 kWh/kg in DC-CDI and 9.763 kWh/kg in pulsed-CDI.

In the paper of Cunping Huang [28], although the principle of electrolysis and capacitive deionization was different, the mass transfer of them was very similar. The energy consumption of DC electrolysis and DC pulsed electrolysis coincided with the result of this study. The reason for lower energy consumption of pulsed-CDI may be that, the peak of pulsed current was high enough to achieve the same removal rate as the DC current, but the unloaded stage of the pulsed current (off-time) could save energy. Although the difference of energy consumption was not much, in the long run, energy conservation in pilot-scale experiment would be more than that in lab-scale experiment.

3.2. Operating parameters of the pulsed power supply in CDI

3.2.1. Duty cycle

Duty cycle determines the ratio of loaded phase (on-time) and unloaded time (off-time) in a pulsed cycle. In Fig. 8, in the treatment of NO_3^- water (initial concentration was 40 mg/L), under a frequency of 10^4 Hz , duty cycle of 20%, 50%, 80% were compared. After 60 min, the remaining concentration of NO_3^- were 19.4 mg/L, 12.24 mg/L, 15.12 mg/L, respectively. A too high or too low duty cycle wasn't conducive to mass transfer. As for duty cycle of 20%, the loaded phase was 0.002 s, and the unloaded phase was 0.008 s. The action time of the electric field was too short, in essence, the capacitive deionization had been weakened. While as for duty cycle of 80%, the pulsed current was nearly to DC current (duty cycle of 100%), and the characteristics of pulsed current weren't obvious. So the duty cycle of 50% was optimal in pulsed-CDI.

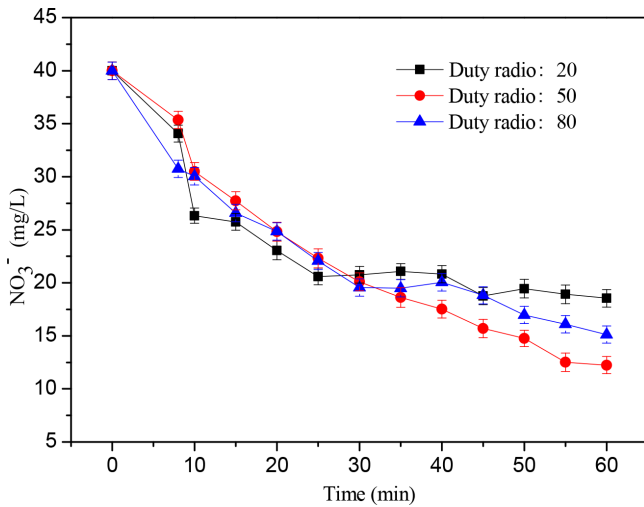


Fig. 8. Duty cycle effect on removal rate of NO_3^- (frequency: 10^3Hz)

3.2.2. Frequency

Frequency is the derivative of the pulse period, and the length of a pulse period is derived by frequency; the larger the frequency is, the shorter the pulse period becomes. The frequency of 10^2 , 10^3 , 10^4 , 10^5 Hz were compared, and took $C_{\text{NO}_3^-}/C_0$ as criterion. $C_{\text{NO}_3^-}$ was the concentration of NO_3^- , and C_0 was the initial concentration. In Fig. 9, the frequency of 10^4 Hz was optimal. From the frequency of 10^2 – 10^4 Hz, $C_{\text{NO}_3^-}/C_0$ decreased with the increasing frequency, however, at the frequency of 10^5 Hz, $C_{\text{NO}_3^-}/C_0$ was maximum, and the removal rate of NO_3^- was minimum. In pulsed-CDI, there was an optimal frequency for each ion. Next, the deformation of ionic atmosphere was used to discuss the impact of frequency of pulse electric field on aqueous solution.

In aqueous solution, positive and negative ions exist in the form of hydrated ions, so the movement of charged ions will drive the movement of hydrated ions. According to ionic atmosphere in Debye-Hückel theory, the ions in the solution could be regarded as composed of several

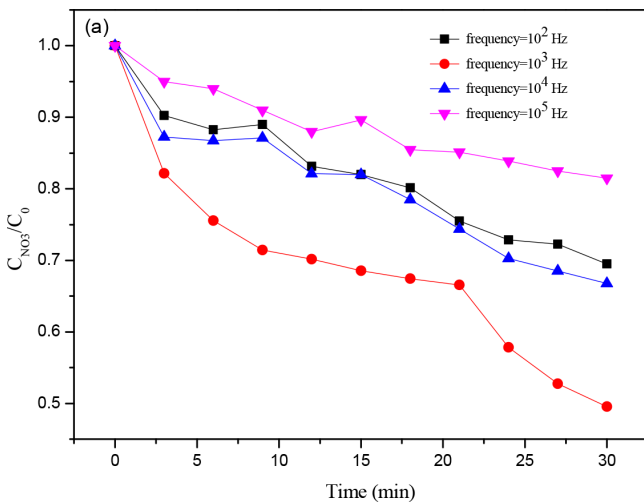


Fig. 9. Frequency effect on removal rate (duty cycle: 50%). (a) NO_3^- .

ionic atmospheres, and the interaction between each ionic atmosphere is zero. When the applied electric field is a constant electric field, the central ions and the ionic atmosphere would move in the opposite direction. When the central ions continue to move until they are removed from the boundary of the ionic atmosphere, the electric balance of the ionic atmosphere is destroyed. It would be necessary to redistribute both the central ions and the opposite ionic atmosphere around them, in an attempt to achieve a new electrical equilibrium.

The movement of the central ion out from the ionic atmosphere would cause the ionic atmosphere to rearrange, as well as other coordinated water molecules. The effect of ion rearrangement is enormous. The key condition for such a disturbance is that the central ion moves out from the ionic atmosphere. In pulsed-CDI, the ion atmosphere move periodically with the periodic change of the pulsed electric field. According to the different motion state of ionic atmosphere, it can be divided into three cases. The three cases are:

- (1) When the frequency of pulsed electric field is low, the central ions in the ionic atmosphere could move from the ionic atmosphere, resulting in a large range of ions rearrangement, which has a greater impact on the solution system;
- (2) If the frequency rises to a certain value, which means in one cycle, the central ions only move a distance to reach the edge of the ionic atmosphere, and the distance equals to the radius of ionic atmosphere. In this case, the movement and rearrangement is greater than that at low frequencies, which would cause greater disturbance. The disturbance to solution reaches the maximum.
- (3) If the frequency continues to rise, the central ions could not move out of the ionic atmosphere, then the central ions in the ionic atmosphere could only reciprocate within the ionic atmosphere. At this time, compared with the above two cases, the ions would not impact on the solution significantly. The higher the frequency is, the smaller the amplitude of motion.

Based on the second case, the frequency should be equal to the reciprocal of the time, from which the central ion moves from the center to the edge of the ionic atmosphere. We assumed the velocity of the central ion and the ion with opposite charges are V_1 , V_2 , a is the ionic radius of the central ion, the frequency (f_0) could be expressed as Eq. (6):

$$(v_1 + v_2) \times \frac{1}{f_0} = \frac{1}{\kappa} \quad (6)$$

In Eq. (6), $1/\kappa$ is the radius of ion atmosphere as Eq. (7):

$$\kappa^2 = \frac{4\pi\epsilon^2}{DKT} \cdot \frac{N}{1000} \cdot \sum_i c_i z_i^2 \quad (7)$$

D : dielectric constant; k : Boltzmann constant, 1.386×10^{-16} ; T : thermodynamic temperature; N : Avogadro constant, 6.024×10^{23} ; C_i : concentration of i ion; Z_i : valence of i ion.

In Eq. (6), V_i could be expressed as Eq. (8):

$$v_i = u_i \cdot E \tag{8}$$

u_i : ion mobility; E : electric field intensity.

From Eqs., (6) and (7), optimal frequency (f_0) is related to properties of ion, such as: ionic radius, valence, ion mobility, and also related to the concentration of ion.

Taking a NaNO_3 with a concentration of 40 mg/L as example, the radius of ionic atmosphere was calculated under the condition of 1.5 V electric field voltage and 2 mm plate spacing; the ionic mobility was found as follows: Na^+ : $5.19 \times 10^{-8} \text{ m}^2 + \text{v}^{-1} + \text{s}^{-1}$; NO_3^- : $7.4 \times 10^{-8} \text{ m}^2 + \text{v}^{-1} + \text{s}^{-1}$. As Eq. (7), the radius of the ionic atmosphere was equal to $5.3417 \times 10^{-10} \text{ m}$, and took 5.3417×10^{-10} into Eq. (6), f_0 was equal to 1531 Hz, which corresponds to 1000 Hz in experimental result. It shows that this method has certain application value.

3.3. Molecular dynamics simulation

3.3.1. Radial distribution function

After achieving dynamic balance, we got the radial distribution function of Na^+ around the graphite sheet under the DC electric field, the pulsed electric field of 5 GHz, 1 THz and 10 THz. As shown in Fig. 10, in the pulsed electric field of 5 GHz, the peaks of Na^+ were found at 2.09 Å, 3.33 Å, and 4.06 Å and the maximum peak was at 2.09 Å. Although there was a peak at 2.09 Å under the DC electric field, it was slightly less. At 4.06 Å, it was the main component of adsorption under the DC electric field. In the pulsed electric field of 1 THz and 10 THz, the adsorption of Na^+ were similar to that in the DC electric field, but the performances were worse. It could be seen that, in the pulsed electric field of 5 GHz, the position of the adsorbed Na^+ was closer to the graphite sheet than any other electric field. This result was consistent with that in 3.1, and the removal rate by pulsed-CDI was better than DC-CDI. The effect of concentration polarization and the migration resistance from solution to the EDL were reduced [17].

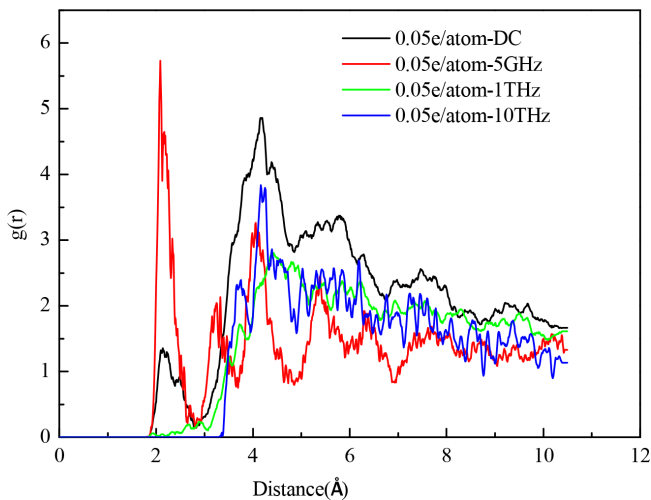


Fig 10. Radial distribution function (RDF) of Na^+ around the graphite sheet.

3.3.2. Orientation distribution

As shown in Fig. 11, between 10 Å and 65 Å, the average distribution of hydrogen and oxygen atoms was relatively

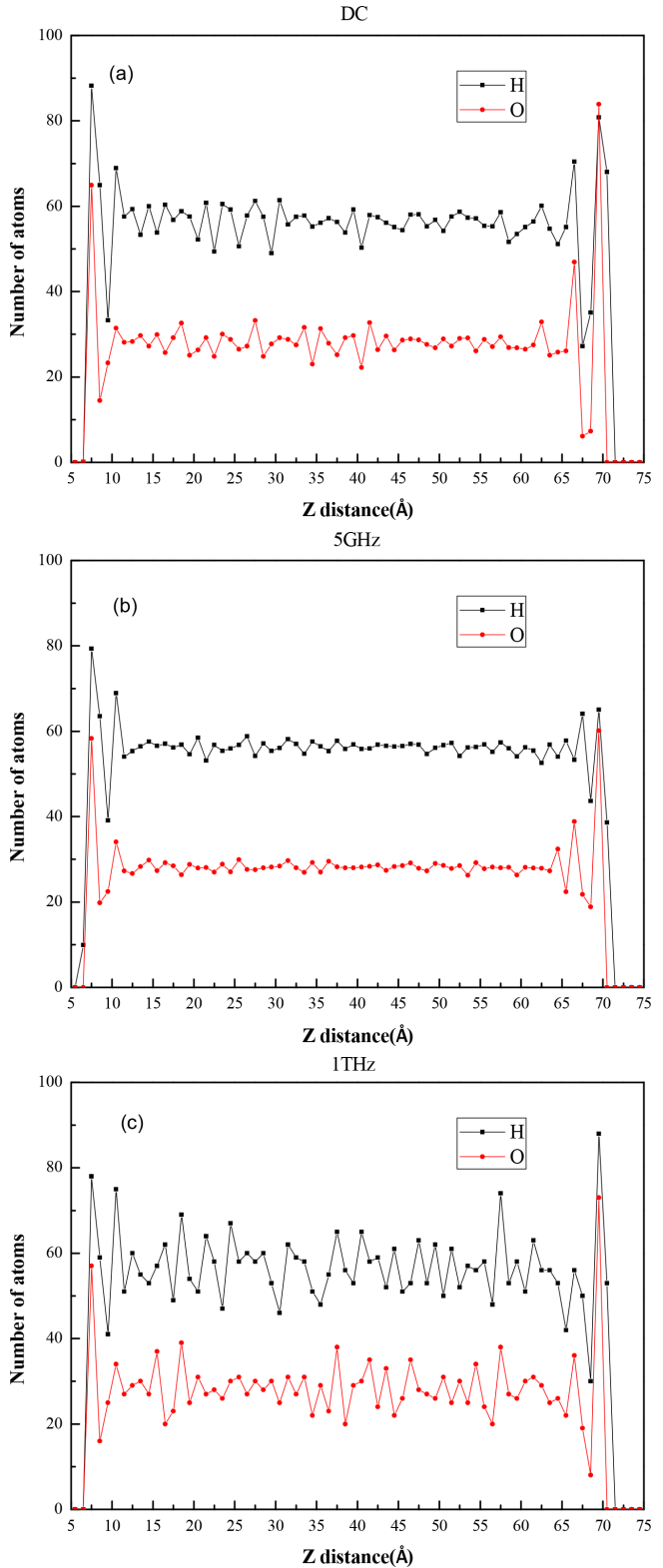


Fig 11. Orientation distribution of H and O, (a): DC, (b): 5 GHz, (c): 1 THz.

gentle, and there was no larger proportion of atoms in a certain place. The water molecules in this area could be seen as bulk water. While at the areas of 0 Å to 10 Å and 65 Å to 75 Å, there was a big fluctuation in the average distribution. As shown in Table 1, the oxygen atoms at 7.5 Å and hydrogen atoms at 69.5 Å, 70.5 Å were the majority in that layer. In these areas, the water molecules were the polarized water. But compared to the DC electric field and the pulsed electric field of 1 THz, the average distribution of hydrogen atom and oxygen atom at 69.5 Å, 70.5 Å in 5 GHz was much gentler. We speculated that, it was because of the intermittent load of pulsed electric field. During the unloaded stage of pulsed current, the dipole moment of polarized water molecule tended to return to an undirected state under the drive of thermal motion. But the relaxation time of dipole moment limited this trend, which meant, if the time of the unloaded stage was shorter than the relaxation time of dipole moment, the dipole moment hadn't recovered yet, while the next loaded stage was coming again. In this study, the unloaded stage of pulsed electric field of 5 GHz was long enough to let the dipole moment recover, so the orientation polarization of water molecules was weakened. But for the frequency of 1 THz, the frequency was too large, and the time of one cycle was too short. The orientation polarization existed all the time.

3.3.3. System potential energy

We calculated the change of system potential energy as Na^+ moved. We intercepted a part of potential energy change to illustrate the problem. As shown in Fig. 12, under

Table 1
Average distribution of hydrogen and oxygen atoms at the points of 7.5 Å, 69.5 Å, 70.5 Å

Distance	Atom	DC	5 GHz	1 THz
7.5 (Å)	O	64.9	58.2	57
7.5 (Å)	H	88.2	79.3	78
69.5 (Å)	O	83.9	60.1	73
69.5 (Å)	H	80.8	65	88
70.5 (Å)	H	68	38.6	53

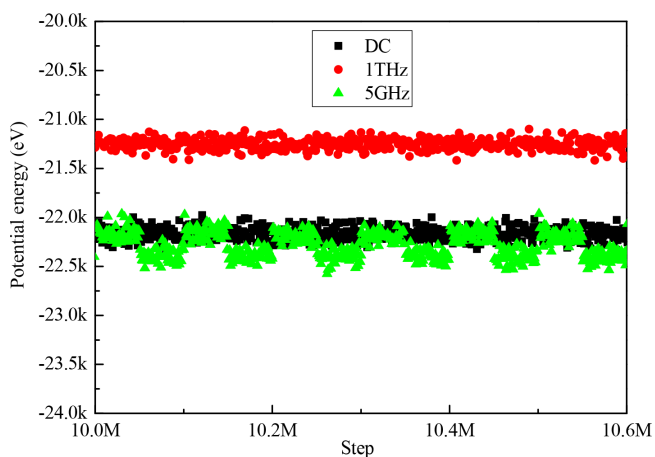


Fig. 12. Change of system potential energy as Na^+ moves.

the pulsed electric field of 5 GHz, the change of potential energy was similar to the waveform of pulse current. At the loaded stage, the potential energy of the system was equivalent to that in DC field, and the potential energy decreased about 0.25 eV at the unloaded stage. While under the pulsed electric field of 1 THz, the potential energy of the system was roughly constant and always higher than the other two. Combined this result with that in 3.2.2, not all pulsed electric field of any frequency are suitable for pulsed-CDI, and optimal frequency is related to properties of ion, concentration of ion.

4. Conclusions

The optimal duty cycle and frequency in pulsed-CDI were investigated. By contrast, duty cycle of 50% was optimal. A frequency of 1000 Hz was suitable for NO_3^- of initial concentration 40 mg/L. optimal frequency (f_0) is related to properties of ion, such as: ionic radius, valence, ion mobility, and also related to the concentration of ion.

The results of molecular dynamics simulation were consistent with the experimental results. The reasons for excellent performances of pulsed-capacitive deionization in desalination may be that: the effect of concentration polarization and the migration resistance from solution to the EDL were reduced

Acknowledgments

This work was supported by the National Natural Science Foundation of China (Nos. 51678118).

References

- [1] Y. Oren, Capacitive deionization (CDI) for desalination and water treatment—past, present and future (a review), *Desalination*, 228 (2008) 10–29.
- [2] Y. Zhao, X.M. Hu, B.H. Jiang, L. Li, Optimization of the operational parameters for desalination with response surface methodology during a capacitive deionization process, *Desalination*, 336 (2014) 64–71.
- [3] M.E. Suss, S. Porada, X. Sun, P.M. Biesheuvel, J. Yoon, V. Presser, Water desalination via capacitive deionization: what is it and what can we expect from it? *Energy Environ. Sci.*, 8 (2015) 2296–2319.
- [4] Y. Liu, C.Y. Nie, X.J. Liu, X.T. Xu, Z. Sun, L.k. Pan, Review on carbon-based composite materials for capacitive deionization, *RSC Adv.*, 5 (2015) 15205–15225.
- [5] H. Yoon, J. Lee, S. Kim, J. Yoon, Hybrid capacitive deionization with Ag coated carbon composite electrode, *Desalination*, 422 (2017) 42–48.
- [6] W.S. Cai, J.B. Yan, T. Hussin, J.Y. Liu, Nafion-AC-based asymmetric capacitive deionization, *Electrochim. Acta*, 225 (2018) 407–415.
- [7] J. Ma, L. Wang, F. Yu, Water-enhanced performance in capacitive deionization for desalination based on graphene gel as electrode material, *Electrochim. Acta*, 263 (2018) 40–46.
- [8] C.J. Feng, C.C. Tsai, C.Y. Ma, C.P. Yu, C.H. Hou, Integrating cost-effective microbial fuel cells and energy-efficient capacitive deionization for advanced domestic wastewater treatment, *Chem. Eng. J.*, 330 (2017) 1–10.
- [9] L.L. Yuan, X.F. Yang, P. Liang, L. Wang, Capacitive deionization coupled with microbial fuel cells to desalinate low-concentration salt water, *Bioresour. Technol.*, 110 (2012) 735–738.

- [10] A. Hassanvand, G.Q. Chen, P.A. Webley, S.E. Kentish, A comparison of multicomponent electro sorption in capacitive deionization and membrane capacitive deionization, *Water Res.*, 131 (2018) 100–109.
- [11] K.S. Lee, Y.H. Cho, K.Y. Choo, S.C. Yoon, M.H. Han, D.K. Kim, Membrane-spacer assembly for flow-electrode capacitive deionization, *Appl. Surf Sci.*, 433 (2018) 437–442.
- [12] S.C. Yang, H.K. Kim, S. Jeon, J.Y. Choi, J.G. Yeo, H.R. Park, J. Jin, D.K. Kim, Analysis of the desalting performance of flow-electrode capacitive deionization under short-circuited closed cycle operation, *Desalination*, 423 (2017) 110–121.
- [13] P. Nativ, O. Lahav, Y. Gendel, Separation of divalent and monovalent ions using flow-electrode capacitive deionization with nanofiltration membranes, *Desalination*, 425 (2018) 123–129.
- [14] A.A. Marc, C.L. Ana, P. Jesus, Capacitive deionization as an electrochemical means of saving energy and delivering clean water. Comparison to present desalination practices: Will it compete? *Electrochim. Acta*, 55 (2010) 3845–3856.
- [15] U. Emekli, C. Alan, Effect of additives and pulse plating on copper nucleation onto Ru, *Electrochim. Acta*, 54 (2009) 1177–1183.
- [16] F.F. Xia, J.Y. Tian, Effect of plating parameters on the properties of pulse electro deposited Ni–TiN thin films, *Ceram. Int.*, 42 (2016) 13268–13272.
- [17] P. Sistat, P. Huguet, B. Ruiz, G. Pourcelly, Effect of pulsed electric field on electro dialysis of a NaCl solution in sub-limiting current regime, *Electrochim. Acta*, 164 (2015) 267–280.
- [18] C.A. Nicolás, P. Gérald, L. Bazinet, Impact of pulsed electric field on electro dialysis process performance and membrane fouling during consecutive demineralization of a model salt solution containing a high magnesium/calcium ratio, *J. Colloid Interface Sci.*, 361 (2011) 79.
- [19] C.A. Nicolás, P. Gérald, L. Bazinet, Water splitting proton-barriers for mineral membrane fouling control and their optimization by accurate pulsed modes of electro dialysis, *J. Colloid Interface Sci.*, 447 (2013) 433–441.
- [20] K. Sharma, R.T. Mayes, J. Kiggans Jr, S. Yiaccoumi, H.Z. Bilheux, L.M.H. Walker, D. DePaoli, S. Dai, C. Tsouris, Enhancement of electro sorption rates using low-amplitude, high-frequency, pulsed electrical potential, *Sep. Purif. Technol.*, 129 (2014) 18–24.
- [21] J.W. Feng, H.M. Ding, Y.Q. Ma, Water desalination by electrical resonance inside carbon nanotube, *Phys. Chem. Chem. Phys.*, 18 (2016) 28290–28296.
- [22] G.W. Sun, D.H. Long, X.J. Liu, W.M. Qiao, Asymmetric capacitance response from the chemical characteristics of activated carbons in KOH electrolyte, *J. Electroanal. Chem.*, 659 (2011) 161–167.
- [23] S. Plimpton, Fast parallel algorithms for short-range molecular dynamics, *J. Comput. Phys.*, 117 (1995) 1–19.
- [24] P. Bjelkmar, P. Larsson, M.A. Cuendet, B. Hess, E. Lindahl, Implementation of the CHARMM force field in GROMACS: analysis of protein stability effects from correction maps, virtual interaction sites, and water models, *J. Chem. Theory Comput.*, 6 (2010) 459–446.
- [25] W.L. Jorgensen, J. Chandrasekhar, J.D. Madura, R.W. Impey, M.L. Klein, Comparison of simple potential functions for simulating liquid water, *J. Chem. Phys.*, 79 (1983) 926–935.
- [26] K.F. Rinne, S. Gekle, D.J. Bonthuis, R.R. Netz, Nanoscale pumping of water by AC electric fields, *Nano Lett.*, 12 (2012) 1780–1783.
- [27] R.W. Hockney, J.W. Eastwood, *Computer Simulation Using Particles*, Adam Hilger Ltd, Bristol, 1981.
- [28] C.P. Huang, Solar hydrogen production via pulse electrolysis of aqueous ammonium sulfite solution, *Sol Energy*, 91 (2013) 394–401.